COMPUTATIONAL MODELING OF RESIDUAL STRESSES IN SIMULTANEOUS TURNING PROCESS

Faisal Hassan [1,a)] and Kalidasan Rathinam[2,b)]

[1] Lovely Professional University, Punjab, India
[2] Lovely Professional University, Punjab, India

Abstract. Residual stresses play a vital role in determining the quality of the turned components. Numerical modelling of residual stresses provides a deep insight of the process mechanism and increases the productivity by conserving time, material and manpower. In simultaneous turning process, two tools are engaged simultaneously to perform the turning process. In this paper numerical investigation was performed to determine the effect of chamfer angle and chamfer width for various feeds on the surface residual stresses. The numerical simulation was done using commercially available software ABAQUS 6.14. The work and tool material are AISI 4340 steel and carbide. CPE4RT four node plane strain element was used for the analysis. A Johnson-Cook damage criterion was employed for the chip separation. The friction between the chip and the cutting tool was based on penalty contact approach. The coefficient of friction was taken as 0.3. With the increase in chamfer angle and chamfer width, the surface residual stresses increases. This is attributed to the increase in cutting forces and plastic strain. At constant chamfer angle, with increase in cutting speed the cutting forces remain constant for both the cutting tools. The same trend was also observed for the chamfer width. On the whole, the usage of chamfered cutting tools proved to be beneficial in imparting higher compressive residual stresses in the simultaneous turning process.

Keywords: Chamfer angle, Chamfer width, Residual stress, simultaneous turning, cutting speed, feed.

Nomenclature

V_c	Cutting speed (m/min)
f	Feed (mm/rev)
θ_c	Chamfer angle
W_c	Chamfer width
σ_c^f	Circumferential residual stress of surface machined by first cutting tool
σ_c^s	Circumferential residual stress of surface machined by second cutting tool
σ_a^f	Axial residual stress of the surface machined by first cutting tool
$\sigma^s{}_a$	Axial residual stress of the surface machined by second cutting tool
L	Length of the workpiece (mm)
H	Height of the workpiece (mm)
A	Initial yield stress (MPa)
B	Hardening modulus (MPa)
C	Strain rate dependency coefficient (MPa)
D	Damage parameter
P	Hydrostatic pressure (MPa)
n	Work hardening coefficient
m	Thermal softening parameter
$D_1D_2D_3D_4D_5$	Failure constants
$\bar{\sigma}$	Flow stress (MPa)
$\bar{\varepsilon}$	Equivalent plastic strain
$\dot{\bar{\varepsilon}}$	Plastic strain rate (s^{-1})
$\dot{\bar{\varepsilon}}_0$	Reference strain rate (s^{-1})
θ	Process temperature (˚C)
$\theta_{melting}$	Melting temperature of work material (˚C)
θ_{room}	Ambient temperature (˚C)
$\Delta\bar{\varepsilon}$	Increment of equivalent plastic strain
$\bar{\varepsilon}_f$	Equivalent strain at failure

1 Introduction

Metal cutting technologies are witnessing a rapid development in various fields such as computational modelling, tool materials, high material removal rate and better surface finish. These factors lead to higher productivity and superior product quality. Fatigue life of the turned components is one of the important quality parameter for rotational shafts, gears, axles and other parts that are subjected to fluctuating reversal loads. A method of increasing the fatigue life of rotary components is by inducing higher compressive residual stresses during the turning process. Fatigue life and productivity can be increased by turning with two tools simultaneously. The process parameters such as cutting speed, feed, rake angle, nose radius, chamfer angle, chamfer width plays an important role in inducing the residual stresses on the turned component. Several researchers had investigated this aspect. Hirao *et al.* (1982) determined the effect of cutting edge chamfer angle and chamfer length on cutting and feed forces. The cutting tool and workpiece materials used were carbide and 4340 and 1045 steel. Cutting and thrust forces were measured for chamfer angles of 22°, 41° and 60° for different chamfer lengths. It was found that chamfer

angle had significant influence on thrust force and negligible effect on cutting force. Fuh & Chang (1995) [2] proposed a new cutting model of various tool geometries with a chamfered main cutting edge. The theoretical and the experimental values of the cutting forces predicted by this model were found to be consistent with each other. The chamfered cutting edge reduces the cutting forces and improves the surface roughness of the workpiece. Ren & Altintas (2002) [3] proposed an analytical model to examine the effect of chamfer angle and other process variables on the cutting forces. The workpiece material used was P20 mold steel and two different chamfered cutting tool materials of carbide and CBN were used. It was observed that the optimal chamfer angle is -15° and the cutting speed is 240m/min for carbide tools. For CBN tools, the cutting speed can be increased up to 600m/min. Movaheddy et al.(2002) [4] performed the numerical simulation of the machining process with pointed, blunt and chamfered edges for carbide and CBN tools. ALE approach was used to examine the tool-edge geometry on the chip formation process. It was found that the cutting forces increase with the increase in chamfer angle. Zhou et al.(2003) [5] studied the effect of chamfer angle on the wear of PCBN tool material in hard turning process. It was found that the cutting forces increase with the increase in chamfer angle. The tool life was found maximum for the chamfer angle 15° and minimum for the chamfer angle 30°. Ozel et al. (2004) [6] studied the effect of various parameters like cutting tool geometry, cutting speed, feed and workpiece hardness on the forces in hard turning of AISI H13 steel. The results obtained shows that the cutting and feed force components were affected by cutting speed, cutting edge geometry and workpiece hardness. Small edge radius and lower workpiece hardness results in lower tangential and radial forces. Choudhury and Zukhairi (2005) [7] performed the interrupted and continuous turning process of medium carbon low alloy steel using chamfered tools. The chamfer widths and chamfer angles were varied and it was found that with the increase in the chamfer width, the cutting forces and feed forces increases. Similarly with the increase of chamfer angle, the cutting forces increased but when the chamfer angle is maximum, the cutting and feed forces were found to be low. Kurt and Seker (2005) [8] investigated the effect of chamfer angle on the cutting forces and stresses in turning process using the finite element software ANSYS. The work material used was AISI 52100 bearing steel and the cutting tool was polycrystalline cubic boron nitride. It was found that the cutting forces and stresses increased with the increase in chamfer angle. Klocke and Kratz (2005) [9] studied the influence of PCBN cutting tool geometry both experimentally and by numerical simulation for hard turning process. It was monitored that the cutting edges of the tool failed abruptly due to excessive crater wear which reduces the strength of the cutting tool. Karpat and Ozel (2008) [10] investigated the tool-chip frction characteristics of curvilinear PCBN tools with different edge geometries on AISI 4340 steel. Finite element simulations were used to study temperature, strain and stress distributions in the cutting tool. It was found that as edge radius increases, strains and temperature on the machined surface increases. Khalili and Safaei (2009) [11] performed the machining of a mild carbon low alloy steel by a carbide tool using finite element analysis. The effect of chamfer width and chamfer angle was studied on various process variables like force, stress and temperature. It was found that with the increase in chamfer width or chamfer angle, the cutting and thrust forces increases. For a constant chamfer width, as the cutting speed increases, the tool temperature is elevated. Sahoo and Sahoo (2012) [12] investigated the cutting forces, surface roughness and chip morphology in the hard turning of AISI 4340 steel using uncoated and multilayer coated carbides at high cutting speeds. The results showed that the tool life for multilayer coated carbides was higher than the uncoated carbides. Also, the forces generated using uncoated carbide were higher than the multilayered and single coated tools. Li et al. (2017) [13] performed the high speed hard-turning of bearing steel using PCBN tools with negative chamfered arc edge and sine-strengthened edge. It was observed that the cutting forces of the sine-strengthened edge were smaller than the negative chamfered edges. Chen et al (2018) [14] carried out the high-speed hard cutting of hardened steel by PCBN tools with variable and uniform chamfered edge to obtain the variation of cutting force, chip morphology and tool wear with cutting time. It was observed that the radial and axial forces generated by the tools with variable chamfered edge were less as compared to uniform chamfered edge. The chips formed by variable chamfered edge tools remained wavy while as those of uniform chamfered edge tools were curvilinear. Gao et al (2018) [15] studied the effect of different chamfered cutting edges of micro mill on the tool cutting performance. Slot milling experiments were performed on aluminium 7075 with the help of micro mills of various chamfer lengths. The results obtained showed that with the increase in chamfer length, the life of tool increases. But the width of flank wear also increases because of high stresses generated in the cutting zone. Liu et al. (2018) [16] investigated the influence of tool wear and cutting speed of variable chamfer PCBN insert and fixed chamfer PCBN insert on the machined surface of bearing steel. It was found that the cutting forces produced by the variable chamfer tool was less as compared to the fixed chamfer tool. Also, better surface roughness can be obtained by using the variable chamfer tool.

It can be seen from the above literature that a lot of work has been done on conventional and double tool turning process in the aspect of experimentation, numerical modelling and optimisation. In the case of chamfered tools, the work reported in the above literature is limited to single tool turning process. The work done on the chamfered tools in case of double tool turning is not done up to now. The aim of the present work is to numerically study the effect of chamfer angle and chamfer width on the surface residual stresses induced on the machined surface for various feeds in simultaneous turning process.

Fig.1 shows the schematic of simultaneous turning process with chamfered cutting tool.

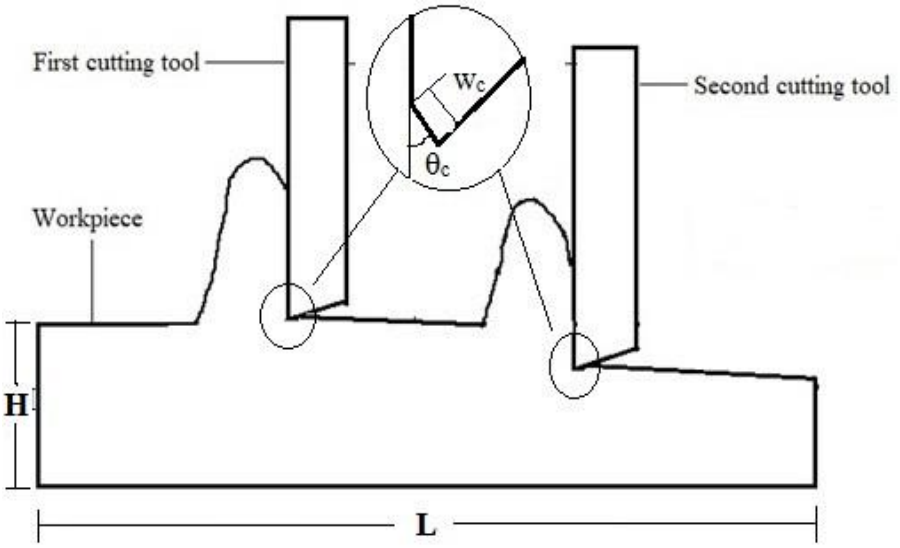

Fig. 1. Schematic view of simultaneous turning process with chamfered cutting tool

2 Numerical Model

2.1 Geometric and Material Model

A 2D orthogonal cutting model is created using ABAQUS 6.14 software. The workpiece is of rectangular cross-section with length 2 mm and height 0.4 mm. The cutting tool is of 0.2 mm width and 0.8 mm height. The material used for the cutting tool is uncoated carbide and the workpiece is AISI 4340 steel. The Johnson-Cook material model is used for the simulation of the cutting process. The Johnson-Cook parameter for the workpiece material AISI 4340 steel is shown in Table 1.

Table 1 Johnson-Cook parameters for AISI 4340 steel

A	B	C	N	m	D_1	D_2	D_3	D_4	D_5
792	510	0.014	0.26	1.03	0.05	3.44	-2.12	0.002	0.610

The flow stress is given by

$$\bar{\sigma} = (A + B\bar{\varepsilon}^{n})\left[1 + C\ln\left(\frac{\dot{\bar{\varepsilon}}}{\dot{\bar{\varepsilon}}_0}\right)\right]\left[1 - \left(\frac{\theta-\theta_{room}}{\theta_{melting}-\theta_{room}}\right)^{m}\right] \quad (1)$$

The chip formation and separation is obtained by equivalent plastic strain rate criterion. Its critical value determines the material failure. The material damage parameter is given by

$$D = \Sigma\left(\frac{\Delta\bar{\varepsilon}}{\bar{\varepsilon}_f}\right) \quad (2)$$

The equivalent plastic strain is given by

$$\bar{\varepsilon}_f = \left[D_1 + D_2\exp\left(D_3\frac{P}{\bar{\sigma}}\right)\right]\left[1 + D_4\ln\left(\frac{\dot{\bar{\varepsilon}}}{\dot{\bar{\varepsilon}}_0}\right)\right]\left[1 + D_5\left(\frac{\theta-\theta_{room}}{\theta_{melting}-\theta_{room}}\right)\right] \quad (3)$$

2.2 Explicit Dynamic Analysis

Explicit dynamic analysis is used in those cases which are non-linear and involve large deformations and contact change like machining process. It uses an integration technique based on central difference method. Also, it does not require convergence and hence lesser disk space is required for obtaining the solution.

2.3 Contact Modelling

The kinematic contact method is used to enforce the contact constraints between the rake surface of the cutting tool and the chip surface. For this purpose, penalty contact with constant coefficient of friction is used.

2.4 Mesh and Boundary Conditions

Four node plain strain bilinear with temperature and displacement, CPE4RT quadrilateral elements are used in this work. The workpiece consists of elements and nodes. The workpiece is kept fixed and the bottom surface of workpiece is kept fixed. Both the cutting tools are constrained along y-directions and the cutting velocity are provided along x-directions. The simulation was performed for the chamfer widths of 0.10 mm, 0.15 mm and 0.20 mm and chamfer angles of 10°, 30° and 50°. The feeds taken are 0.10 mm/rev, 0.15 mm/rev and 0.20 mm/rev. The cutting velocity is taken 150 m/min and the distance between the cutting tools is kept constant equal to 1 mm.

3 Numerical Results and Discussions

The results of the developed finite element model are presented in this section. The influence of chamfer angle, chamfer width and feed on the circumferential and axial residual stresses of the surfaces machined by first and second cutting tool is reported in the following subsections:

3.1 Effect of chamfer angle

On Residual Stresses

Figure represents the variation of surface residual stresses machined by the first and second cutting tool for different chamfer angles for the cutting speed of 150 m/min and feed ---. It can be observed that both the circumferential and axial compressive residual stresses increased with the increase in chamfer angle for the surfaces machined by first and second cutting tool.

For a chamfer angle of 10˚, the circumferential and axial compressive residual stresses of the surface machined by the first cutting tool are 586 MPa and 260 MPa respectively. It is obtained for a chamfer width of 0.2 mm and 0.1 mm/rev feed. When the chamfer angle is increased to 30˚, the circumferential and axial compressive residual stresses increased by 54% and 95% respectively. On further increasing the chamfer angle from 30° to 50°, the circumferential and axial compressive residual stresses increased by 18% and 55% respectively. Similarly, the circumferential and axial compressive residual stresses of the surface machined by the second cutting tool are 454 MPa and 456 MPa respectively. When the chamfer angle is increased to 30˚, the circumferential and axial compressive residual stresses increased by 84% and 83% respectively. On further increasing the chamfer angle from 30° to 50°, the circumferential and axial compressive residual stresses increased by 63% and 25% respectively.

On Cutting and Feed Forces

For a chamfer angle of 10°, the cutting and feed forces generated by the first cutting tool during machining are 540 N and 238 N respectively. When the chamfer angle is increased to 30˚, the cutting and feed forces generated by the first cutting tool during machining are 625 N and 401 N respectively. On further increasing the chamfer angle from 30° to 50°, the cutting and feed forces generated by the first cutting tool during machining are 690 N and 517 N respectively. Similarly, the cutting and feed forces generated by the second cutting tool during machining are 512 N and 226 N respectively. When the chamfer angle is increased to 30˚, the cutting and feed forces generated by the second cutting tool during machining are 608 N and 426 N respectively. On further increasing the chamfer angle from 30° to 50°, the cutting and feed forces generated by the first cutting tool during machining are 646 N and 535 N respectively. It can be observed that the effect of chamfer angle is more dominant on the feed forces as compared to the cutting forces.

3.2 Effect of chamfer width

On Residual Stresses

Figure represents the variation of surface residual stresses machined by the first and second cutting tool for different chamfer widths for the cutting speed of 150 m/min and feed ---. It can be observed that both the circumferential and axial compressive residual stresses increased with the increase in chamfer width for the surfaces machined by first and second cutting tool.

For a chamfer width of 0.1 mm, the circumferential and axial compressive residual stresses of the surface machined by the first cutting tool are 778 MPa and 675 MPa respectively. It is obtained for a chamfer angle of 50° and 0.1 mm/rev feed. When the chamfer width is increased to 0.15 mm, the circumferential and axial compressive residual stresses increased by 29% and 11% respectively. On further increasing the chamfer width from 0.15 mm to 0.2 mm, the circumferential and axial compressive residual stresses increased by 7% and 6% respectively. Similarly, the circumferential and axial compressive residual stresses of the surface machined by the second cutting tool are 969 MPa and 878 MPa respectively. When the chamfer width is increased to 0.15 mm, the circumferential and axial compressive residual stresses increased by 17% and 8% respectively. On further increasing the chamfer width from 0.15 mm to 0.2 mm, the circumferential and axial compressive residual stresses increased by 19% and 9% respectively.

On Cutting and Feed Forces

For a chamfer width of 0.1 mm, the cutting and feed forces generated by the first cutting tool during machining are 624 N and 381N respectively. When the chamfer width is increased to 0.15 mm, the cutting and feed forces generated by the first cutting tool during machining are 647 N and 397 N respectively. On further increasing the chamfer angle from 30° to 50°, the cutting and feed forces generated by the first cutting tool during machining are 688 N and 517 N respectively. Similarly, the cutting and feed forces generated by the second cutting tool during machining are 580 N and 366 N respectively. When the chamfer angle is increased to 30˚, the cutting and feed forces generated by the second cutting tool during machining are 646 N and 491 N respectively. On further increasing the chamfer angle from 30° to 50°, the cutting and feed forces generated by the first cutting tool during machining are 666 N and 535 N respectively.

References

1. Hirao, M., Tlusty, J., Sowerby, R., & Chandra, G. : Chip formation with chamfered tools. Journal of Manufacturing Science and Engineering, Transactions of the ASME, 104(4), 339–342 (1982).
2. K. hua Fuh and C. S. Chang. :Prediction of the cutting forces for chamfered main cutting edge tools. Int. J. Mach. Tools Manuf., vol. 35, no. 11, pp. 1559–1586 (1995).
3. Ren, H., & Altintas, Y. : Mechanics of machining with chamfered tools. Journal of Manufacturing Science and Engineering, Transactions of the ASME, 122(4), 650–659 (2002).
4. Movahhedy, M. R., Altintas, Y., & Gadala, M. S. : Numerical analysis of metal cutting with chamfered and blunt tools. Journal of Manufacturing Science and Engineering, Transactions of the ASME, 124(2), 178–188 (2002).
5. Zhou, J. M., Walter, H., Andersson, M., & Stahl, J. E. : Effect of chamfer angle on wear of PCBN cutting tool. International Journal of Machine Tools and Manufacture, 43(3), 301–305 (2003).
6. Özel, T., Hsu, T. K., & Zeren, E. : Effects of cutting edge geometry, workpiece hardness, feed rate and cutting speed on surface roughness and forces in finish turning of hardened AISI H13 steel. International Journal of Advanced Manufacturing Technology, 25(3–4), 262–269 (2004).
7. Choudhury, I. A., See, N. L., & Zukhairi, M. : Machining with chamfered tools. Journal of Materials Processing Technology, 170(1–2), 115–120 (2005).
8. Kurt, A., & Şeker, U. : The effect of chamfer angle of polycrystalline cubic boron nitride cutting tool on the cutting forces and the tool stresses in finishing hard turning of AISI 52100 steel. Materials and Design, 26(4), 351–356 (2005).
9. Klocke, F., & Kratz, H. : Advanced tool edge geometry for high precision hard turning. CIRP Annals - Manufacturing Technology, 54(1), 47–50 (2005).
10. Karpat, Y., & Özel, T. : Mechanics of high speed cutting with curvilinear edge tools. International Journal of Machine Tools and Manufacture, 48(2), 195–208 (2008).
11. Khalili, K., & Safaei, M. : FEM analysis of edge preparation for chamfered tools. International Journal of Material Forming, 2(4), 217–224 (2009).
12. Sahoo, A. K., & Sahoo, B. : Experimental investigations on machinability aspects in finish hard turning of AISI 4340 steel using uncoated and multilayer coated carbide inserts. Measurement: Journal of the International Measurement Confederation, 45(8), 2153–2165 (2012).
13. Li, S., Chen, T., Qiu, C., Wang, D., & Liu, X. : Experimental investigation of high-speed hard turning by PCBN tooling with strengthened edge. International Journal of Advanced Manufacturing Technology, 92(9–12), 3785–3793 (2017).
14. Chen, T., Guo, J., Wang, D., Li, S., & Liu, X. (2018). : Experimental study on high-speed hard cutting by PCBN tools with variable chamfered edge. International Journal of Advanced Manufacturing Technology, 97(9–12), 4209–4216 (2018).
15. Gao, P., Liang, Z., Wang, X., Li, S., & Zhou, T. : Effects of different chamfered cutting edges of micro end mill on cutting performance. International Journal of Advanced Manufacturing Technology, 96(1–4), 1215–1224 (2018).
16. Liu, X. L., Li, S. Y., Chen, T., & Wang, D. Y. : Research on the Surface Characteristics of Hardened Steel with Variable Chamfer Edge PCBN Insert by High-Speed Hard Turning. International Journal of Precision Engineering and Manufacturing, 19(2), 157–165 (2018).